Countertraveling waves in rotating Rayleigh-Bénard convection

Ligang Li,[1] Xinhao Liao,[1] and Keke Zhang[2]
[1]*Shanghai Astronomical Observatory, Chinese Academy of Sciences, Shanghai 200030, China*
[2]*Department of Mathematical Sciences, University of Exeter, Exeter EX4 4QE, United Kingdom*
(Received 13 November 2007; published 14 February 2008)

Linear and nonlinear counter-traveling waves in a fluid-filled annular cylinder with realistic no-slip boundary conditions uniformly heated from below and rotating about a vertical axis are investigated. When the gap of the annular cylinder is moderate, there exist two three-dimensional traveling waves driven by convective instabilities: a retrograde mode localized near the outer sidewall and a prograde mode adjacent to the inner sidewall with a different wave number, frequency and critical Rayleigh number. It is found that the retrogradely propagating mode is always more unstable and is marked by a larger azimuthal wave number. When the Rayleigh number is sufficiently large, both the counter-traveling modes can be excited and nonlinearly interacting, leading to an unusual nonlinear phenomenon in rotating Rayleigh-Bénard convection.

DOI: 10.1103/PhysRevE.77.027301 PACS number(s): 44.25.+f, 47.55.P-, 05.45.−a

I. INTRODUCTION

Rayleigh-Bénard convection in rotating cylindrical systems heated from below and rotating about a vertical axis has been long studied as a paradigm for understanding the pattern formation effected by the Coriolis force and the general dynamics of rotating fluids (e.g., [1]). The problem is also of geophysical and planetary physical interest, with an application to polar regions in the tangent cylinder of the Earth's and planetary core (e.g., [2]).

There are two geometric parameters in a rotating annular cylinder (Fig 1): the aspect ratio r_o of outer radius $r_o d$ to depth d and the aspect ratio r_i of inner radius $r_i d$ to depth d. The problem of rotating Rayleigh-Bénard convection in cylindrical systems has been extensively studied in two different geometric limits. In the limit $r_i \to 0$, it is now well known that the effect of the sidewall destabilizes convection and the primary bifurcation in the vicinity of the instability threshold takes the form of a retrogradely traveling wave of constant amplitude localized near the sidewall of the cylinder (e.g., [3–6]). It has been shown that the weakly nonlinear retrogradely propagating wave may be described by a single one-dimensional complex Ginzburg-Landau equation for which the coefficients can be determined either by experimental studies (e.g., [7,8]) or by numerical computations (e.g., [5,9]). In the limit $r_i \to \infty$ and $r_o \to \infty$ but with $r_o - r_i = O(1)$ in which the effect of the curvature can be neglected, convection is characterized by two oppositely traveling waves with exactly the same frequencies, wave numbers and critical Rayleigh numbers. In this case, the weakly nonlinear problem may be studied on the basis of two coupled complex Ginzburg-Landau equations (e.g., [10,9]). For a moderate gap $(r_o - r_i) = O(\mathrm{Ta}^{-1/6})$, where Ta is the Taylor number, the two oppositely traveling waves can interfere nonlinearly, leading to various forms of the nonlinear solutions [11].

The intermediate case $r_i = O(1)$ and $r_o = O(1)$, which can also be realized in experiments, has richer dynamics but is mathematically much more complicated in the following way. The curvature effect becomes significant and, consequently, the coupled complex Ginzburg-Landau equations, which are based on expansion in the small amplitude of convection, are, generally speaking, no longer applicable to the problem of nonlinear countertraveling waves. This is because the two oppositely traveling modes are characterized not only by different frequencies and wave numbers, but also, more importantly, by different critical Rayleigh numbers. No linear stability analysis has been carried out for the problem: it is unclear which mode, the retrogradely propagating wave near the outer sidewall or the progradely propagating wave adjacent to the inner sidewall, is convectively more unstable. We also know little about the physical and mathematical properties of the nonlinear countertraveling waves beyond the onset of buoyancy-driven instabilities [12,13]. This Brief Report reports some preliminary results of both the linear analysis of convective instabilities in the form of counter-traveling waves and the corresponding nonlinear solutions in a rotating annular cylinder with $r_i = O(1)$ and $r_o = O(1)$ heated from below and rotating about a vertical axis.

II. MATHEMATICAL FORMULATION

We consider convection in a Boussinesq fluid with constant thermal diffusivity κ, thermal expansion coefficient α and kinematic viscosity ν in an annular cylinder of depth d with inner radius $r_i d$ and outer radius $r_o d$, the geometry of which is shown in Fig. 1. The vertical coordinate, denoted by z, is parallel to the rotation axis, with radial coordinate s and

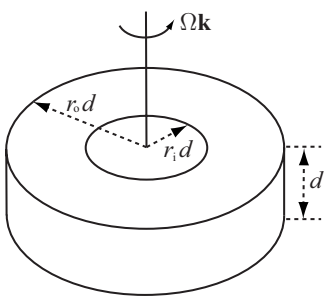

FIG. 1. Geometry of a rotating annular cylinder of depth d with cross section defined by $(r_i d) \le s \le (r_o d)$, s being the distance from the rotation axis.

azimuthal coordinate ϕ. The whole system rotates uniformly with constant angular velocity $\Omega\mathbf{k}$ in the presence of vertical gravity $\mathbf{g}=-g_0\mathbf{k}$, where $\mathbf{k}$ is a vertical unit vector. As in the classical Rayleigh-Bénard problem, the annular cylinder is uniformly heated from below to maintain an unstable vertical temperature gradient, $\nabla\Theta_0=-\beta\mathbf{k}$, where β is a positive constant. The convection problem is governed by the three dimensionless equations

$$\frac{\partial \mathbf{u}}{\partial t}+\mathbf{u}\cdot\nabla\mathbf{u}+\mathrm{Ta}^{1/2}\mathbf{k}\times\mathbf{u}=-\nabla p+R\Theta\mathbf{k}+\nabla^2\mathbf{u}, \quad (1)$$

$$\mathrm{Pr}\left(\frac{\partial\Theta}{\partial t}+\mathbf{u}\cdot\nabla\Theta\right)=\mathbf{u}\cdot\mathbf{k}+\nabla^2\Theta, \quad (2)$$

$$\nabla\cdot\mathbf{u}=0, \quad (3)$$

where

$$R=\frac{\alpha\beta g_0 d^4}{\nu\kappa}, \quad \mathrm{Pr}=\frac{\nu}{\kappa}, \quad \mathrm{Ta}=\frac{4\Omega^2 d^4}{\nu^2},$$

Θ represents the dimensionless deviation of the temperature from its conducting state Θ_0, p is the total pressure, and $\mathbf{u}$ is the three-dimensional velocity field $\mathbf{u}=(u_s,u_\phi,u_z)$ in the cylindrical coordinates (s,ϕ,z) with corresponding unit vectors $(\hat{\mathbf{s}},\hat{\boldsymbol{\phi}},\hat{\mathbf{z}})$. The convection problem is characterized by three nondimensional parameters, the Rayleigh number R, the Prandtl number Pr and the Taylor number Ta.

The boundary conditions are assumed to be no-slip and conducting at the top and bottom

$$u_s=u_\phi=u_z=\Theta=0 \quad \text{at } z=0,\ 1, \quad (4)$$

while the no-slip and insulating sidewalls require that

$$u_s=u_\phi=u_z=\frac{\partial\Theta}{\partial s}=0 \quad \text{at } s=r_i,\ r_o. \quad (5)$$

We shall first perform the stability analysis of linearized versions of Eqs. (1)–(3) subject to the boundary conditions (4) and (5), which provides helpful guidance not only for understanding the phenomenon of countertraveling waves but also for computing the nonlinear interaction of the waves, and then solve the fully nonlinear Eqs. (1)–(3) subject to the boundary conditions (4) and (5) by direct numerical simulations.

III. LINEAR COUNTER-TRAVELING WAVES

It is anticipated that convection in a rapidly rotating annular cylinder is strongly non-axisymmetric (e.g., [3,4]). For the linear stability analysis, a non-axisymmetric velocity vector satisfying Eq. (3) in cylindrical geometry can be expressed in terms of two scalar potentials Ψ and Φ ([14])

$$\mathbf{u}=\frac{1}{s}\frac{\partial\Psi}{\partial\phi}\hat{\mathbf{s}}+\left(\frac{\partial\Phi}{\partial z}-\frac{\partial\Psi}{\partial s}\right)\hat{\boldsymbol{\phi}}-\frac{1}{s}\frac{\partial\Phi}{\partial\phi}\hat{\mathbf{z}}. \quad (6)$$

An important advantage of using (6) is that the two scalar potentials are decoupled in the velocity boundary condition on the two no-slip sidewalls, as well as at the top and bottom bounding surfaces. Making use of the expression (6) and applying $\hat{\mathbf{z}}\cdot\nabla\times$ and $\hat{\mathbf{s}}\cdot\nabla\times$ onto the linearized version of (1), we can derive two independent scalar equations which, together with the linearized (2), are solved numerically by using the Chebyshev-tau method.

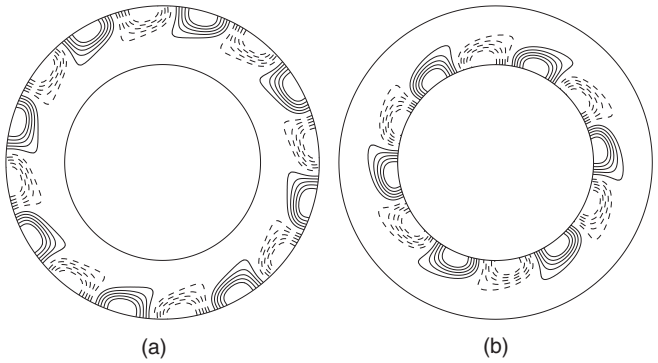

FIG. 2. Two different linear traveling wave solutions for $r_i=1.25$ and $r_o=2.0$: (a) contours of temperature Θ_{out} at $z=1/2$ for the retrogradely traveling mode with $m_o=8, R_o=33\,918$ and $\omega_o=3.967$, and (b) contours of Θ_{in} at $z=1/2$ for the progradely traveling mode with $m_i=6, R_i=35\,563$ and $\omega_i=3.899$.

In the stability analysis, we wish to distinguish two different linear solutions: the first represents the retrogradely propagating wave localized near the outer sidewall, which can be expressed, for example, in the form

$$\Theta_{out}=\Theta_o(s,z,R_o)\exp\{\mathrm{i}m_o\phi+\mathrm{i}\omega_o t\}, \quad (7)$$

where m_o is a positive integer wave number and the Rayleigh number R_o is chosen such that ω_o is positive and real. The second is for the progradely propagating wave adjacent to the inner sidewall,

$$\Theta_{in}=\Theta_i(s,z,R_i)\exp\{\mathrm{i}m_i\phi-\mathrm{i}\omega_i t\}, \quad (8)$$

where m_i is a positive integer wave number and the Rayleigh number R_i is chosen such that ω_i is positive and real.

We are mainly interested in sufficiently large Taylor numbers, $\mathrm{Ta}\gg 1$, for which the convective motions are in the form of traveling waves and tend to concentrate in the vicinities of the sidewalls. Without loss of general physics for rapidly rotating systems, we shall focus on the case $\mathrm{Ta}=10^6$ and $\mathrm{Pr}=7.0$ (water at room temperature) with a fixed $r_o=2$ but taking r_i as a parameter. In the limit $r_i\to 0$, the linear solution is marked by a retrogradely traveling wave concentrating at the outer sidewall, with the Rayleigh number $R_o=33\,918$, azimuthal wave number $m_o=8$, and frequency $\omega_o=3.967$. As r_i increases, for example, to $r_i=1.25$, both the countertraveling modes become realizable: the retrograde mode concentrating at the outer sidewall is still described by the Rayleigh number $R_o=33\,918$ with $m_o=8$ and $\omega_o=3.967$, while the progradely traveling mode concentrated at the inner sidewall is characterized by $R_i=35563$ with $m_i=6$ and $\omega_i=3.899$. The structures of both the countertraveling convective modes are depicted in Fig. 2 for $r_i=1.25$. It is worth noting that, as a result of the wall-localized nature, the spatial structure and critical parameters

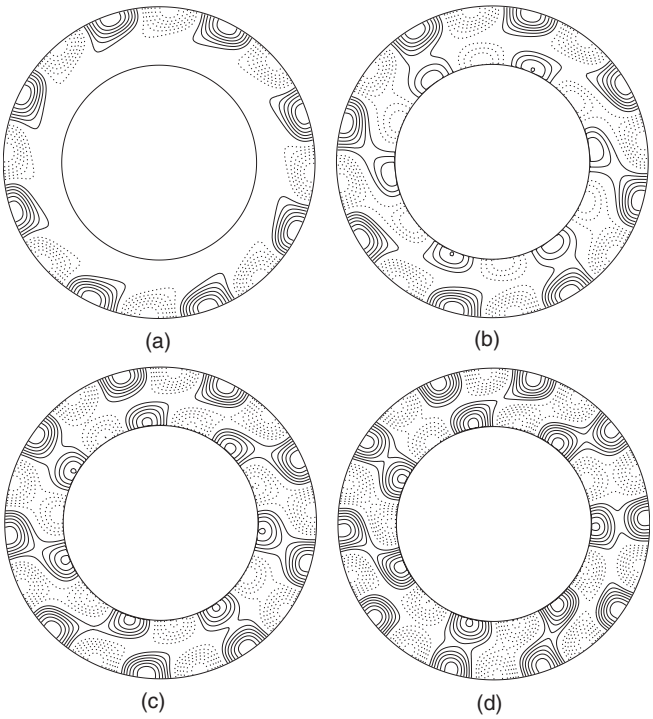

FIG. 3. Snapshots of contours of temperature Θ at $z=1/2$ for nonlinear convection at three different Rayleigh numbers with $r_i=1.25$ and $r_o=2.0$: (a) $R=35\,000$, (b) $R=36\,000$, (c) $R=40\,000$, and (d) $R=50\,000$.

for the retrograde mode remain nearly unchanged for different values of r_i. Our linear stability analysis suggests that $R_i > R_o$ and $m_o > m_i$ for all nonzero r_i and for any sufficiently large Taylor number.

IV. NONLINEAR COUNTER-TRAVELING WAVES

Two features are essential in the understanding of nonlinear countertraveling waves: (i) the effect of the cylindrical curvature destroys the spatial symmetries between the two countertraveling modes, and (ii) the typical radial scale for the wall-localized traveling mode is of $O(\mathrm{Ta}^{-1/6})$ ([6,15,16]), which is of $O(0.1)$ for $\mathrm{Ta}=10^6$. This indicates that the two oppositely traveling waves, obtained for $r_i=1.25$ at $\mathrm{Ta}=10^6$ with different wave numbers and frequencies, have to interact nonlinearly when $R > R_i$. We shall hence focus our study of the nonlinear countertraveling waves on the case $r_i=1.25$.

We choose to tackle the nonlinear problem via direct three-dimensional numerical simulations using a finite difference method. In an attempt to unveil the nature of the bifurcation from convective instabilities, we start the simulations from a Rayleigh number slightly larger than $R_o=33918$. Figure 3 shows the typical spatial structure of the nonlinear waves, representing three different bifurcations at three typical Rayleigh numbers. The primary bifurcation is, as correctly predicted by the linear stability analysis, characterized by a retrogradely traveling wave of constant amplitude localized in the vicinity of the outer sidewall with the dominant azimuthal wave number $m=8$ and frequency about $\omega=4.0$.

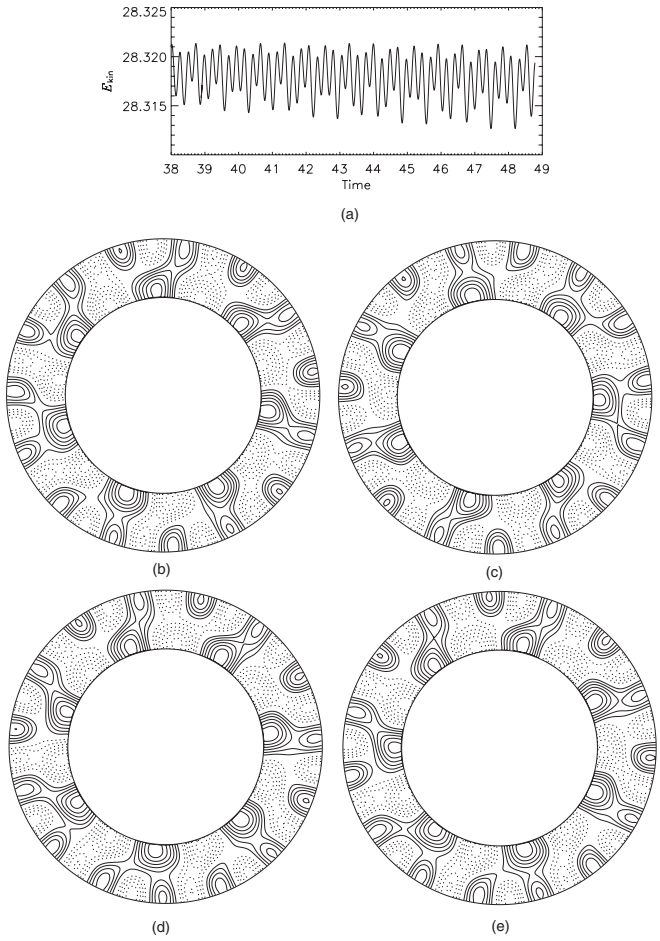

FIG. 4. (a) Kinetic energies of nonlinear countertraveling waves at $R=70\,000$ for $r_i=1.25$ and $r_o=2.0$. (b)–(e) Contours of temperature Θ at $z=1/2$ for four different instants.

This is illustrated in Fig. 3(a) for the nonlinear retrogradely traveling wave obtained at $R=35\,000$.

When the Rayleigh number R increases to 36 000, which is slightly greater than the critical Rayleigh number $R_i=35\,563$ for the progradely traveling mode, the secondary bifurcation takes place. As displayed in Fig. 3(b), both the prograde and retrograde modes with $m_i=6$ and $m_o=8$ are excited, which is consistent with the prediction of the linear stability analysis. This is also consistent with the result of the general symmetry analysis for convection in rotating annulus [17]. When the Rayleigh number R increases to 40 000, which is at 12% above the onset of the least excited wave, the third bifurcation takes place, characterized by the shift of azimuthal wave numbers. The third bifurcation, shown in Fig. 3(c), is marked by the progradely traveling wave in the vicinity of the inner sidewall with a larger wave number $m=7$, a result of the stronger nonlinear effect. At the same time, the dominant wave number of the retrogradely traveling wave is also shifted to $m=9$. Dependent upon the relative phases of the two waves at any instant, two oppositely traveling waves are slipping against each other and nonlinearly interacting, resulting in slight variations of their amplitude. Further bifurcations are generally characterized by a gradual increase of the dominant wave number of the retrogradely

traveling wave, in connection with the mechanism of the Eckhaus-type instability [18]. However, the spatial scale of the progradely traveling wave remains largely unchanged. At $R=50\,000$, for example, the dominant wave number of the retrogradely traveling wave increases to $m=10$, which is depicted in Fig. 3(d).

Kinetic energies of the nonlinear countertraveling waves obtained for $R=7.0\times10^4$, along with their spatial structure at four different instants, are displayed in Fig. 4. The dominant wave number for the retrogradely traveling wave increases to $m=15$ while the wave number of the progradely traveling wave still remains at $m=7$. The two countertraveling waves having different wave numbers and frequencies interfere nonlinearly, creating a unique nonlinear dynamics in rotating Rayleigh-Bénard convection. It is worth mentioning that the onset of rotating Rayleigh-Bénard convection in an infinitely extended layer occurs at $R_c=7.11\times10^4$ for $\mathrm{Ta}=10^6$ and $\mathrm{Pr}=7.0$. It is remarkable that nonlinear rotating convection in the form of countertraveling waves becomes temporally and spatially irregular even before the onset of the classical Rayleigh-Bénard instabilities occurs.

V. SUMMARY AND REMARKS

We have investigated both linear and nonlinear countertraveling waves occurring in a fluid-filled annular cylinder, with realistic no-slip boundary conditions, uniformly heated from below, and rotating about a vertical axis. When the gap of the annular cylinder is moderate, we show that nonlinear solutions are characterized by a retrogradely propagating wave near the outer sidewall and a progradely propagating wave adjacent to the inner sidewall. The two countertraveling modes have different wave numbers, frequencies, and critical Rayleigh numbers. When the Rayleigh number R is sufficiently large, the two countertraveling waves, dependent upon their relative phases at any instant, interact nonlinearly, leading to an unusual nonlinear phenomenon in rotating Rayleigh-Bénard convection. It should be noted that this nonlinear phenomenon is quite different from that in a radially heated annulus (e.g., [19,20]).

It is important to recognize the fundamental difference between the current problem and the annular channel limit $r_i\to\infty$ and $r_o\to\infty$. In the latter case, two oppositely traveling waves have the exactly same frequencies, wave numbers, and critical Rayleigh numbers (e.g., [5,10,9]); they may interact nonlinearly to stick together to form stationary convection [11]. When two countertraveling waves are marked by different wave numbers, frequencies and critical Rayleigh numbers, as in the present study, a stationary convection representing two stuck oppositely traveling waves is no longer possible. Furthermore, it is unlikely that the nonlinear countertraveling waves discussed in this study can be properly described by two coupled complex Ginzburg-Landau equations.

ACKNOWLEDGMENTS

L.L. and X.L. are supported by NSFC Grant Nos. 110310773022 and 10633030, the CAS and 863-Project Grant No. 2006AA01A125. K.Z. is supported by UK NERC and PPARC grants. K.Z. would like to thank F.H. Busse and E. Knobloch for helpful discussions. The numerical computation was supported by Shanghai Supercomputer Center.

[1] M. C. Cross and P. C. Hohenberg, Rev. Mod. Phys. **65**, 851 (1993).
[2] J. M. Aurnou, S. Andreadis, L. Zhu, and P. L. Olson, Earth Planet. Sci. Lett. **212**, 119 (2003).
[3] F. Zhong, R. E. Ecke, and V. Steinberg, Phys. Rev. Lett. **67**, 2473 (1991).
[4] H. F. Goldstein, E. Knobloch, I. Mercader, and M. Net, J. Fluid Mech. **248**, 583 (1993).
[5] E. Y. Kuo and M. C. Cross, Phys. Rev. E **47**, R2245 (1993).
[6] J. Herrmann and F. H. Busse, J. Fluid Mech. **255**, 183 (1993).
[7] Y. Liu and R. E. Ecke, Phys. Rev. Lett. **78**, 4391 (1997).
[8] Y. Liu and R. E. Ecke, Phys. Rev. E **59**, 4091 (1999).
[9] E. Plaut, Phys. Rev. E **67**, 046303 (2003).
[10] M. van Hecke and W. van Saarloos, Phys. Rev. E **55**, R1259 (1997).
[11] K. Zhang, X. Liao, X. Zhan, and R. Zhu Phys. Rev. E **75**, 055302(R) (2007).
[12] J. D. Scheel, M. R. Paul, M. C. Cross, and P. F. Fischer, Phys. Rev. E **68**, 066216 (2003).
[13] E. Serre, E. C. del Arco, and F. H. Busse, in *Nonlinear Dynamics in Fluids*, edited by F. Marqués and A. Meseguer (CIMNE, Barcelona, 2003), pp. 138–140.
[14] F. Marqués, Phys. Fluids A **2**, 729 (1990).
[15] X. Liao, K. Zhang, and Y. Chang, Geophys. Astrophys. Fluid Dyn. **99**, 445 (2005).
[16] X. Liao, K. Zhang, and Y. Chang, J. Fluid Mech. **549**, 375 (2006).
[17] E. Knobloch, Phys. Fluids **8**, 1446 (1996).
[18] T. Benjamin and J. Feir, J. Fluid Mech. **27**, 417 (1967).
[19] E. Plaut and F. H. Busse, J. Fluid Mech. **464**, 345 (2002).
[20] J. Rotvig and C. A. Jones, J. Fluid Mech. **567**, 117 (2006).